HHS Public Access

Author manuscript

Macromol Mater Eng. Author manuscript; available in PMC 2017 May 19.

Published in final edited form as:

Macromol Mater Eng. 2016 August ; 301(8): 935–943. doi:10.1002/mame.201600044.

Self-Cleaning, Thermoresponsive P (NIPAAm-co-AMPS) Double Network Membranes for Implanted Glucose Biosensors

Dr. Ruochong Fei,
Department of Biomedical Engineering, Texas A&M University, College Station, TX 77843-3120, USA

A. Kristen Means,
Department of Materials Science and Engineering, Texas A&M University, College Station, TX 77843-3003, USA

Dr. Alexander A. Abraham,
Department of Biomedical Engineering, Texas A&M University, College Station, TX 77843-3120, USA

Andrea K. Locke,
Department of Biomedical Engineering, Texas A&M University, College Station, TX 77843-3120, USA

Prof. Gerard L. Coté, and
Department of Biomedical Engineering, Texas A&M University, College Station, TX 77843-3120, USA

Center for Remote Health Technologies and Systems, Texas A&M Engineering Experiment Station, College Station, TX 77843-3577, USA

Prof. Melissa A. Grunlan
Department of Biomedical Engineering, Texas A&M University, College Station, TX 77843-3120, USA

Department of Materials Science and Engineering, Texas A&M University, College Station, TX 77843-3003, USA

Center for Remote Health Technologies and Systems, Texas A&M Engineering Experiment Station, College Station, TX 77843-3577, USA

Abstract

A self-cleaning membrane that periodically rids itself of attached cells to maintain glucose diffusion could extend the lifetime of implanted glucose biosensors. Herein, we evaluate the functionality of thermoresponsive double network (DN) hydrogel membranes based on poly(*N*-isopropylacrylamide) (PNIPAAm) and an electrostatic co-monomer, 2-acrylamido-2-methylpropane sulfonic acid (AMPS). DN hydrogels are comprised of a tightly crosslinked,

Correspondence to: Melissa A. Grunlan.

Supporting Information

Supporting Information is available from the Wiley Online Library or from the author.

ionized first network [P(NIPAAm-co-AMPS)] containing variable levels of AMPS (100:0–25:75 wt% ratio of NIPAAm:AMPS) and a loosely crosslinked, interpenetrating second network [PNIPAAm]. To meet the specific requirements of a subcutaneously implanted glucose biosensor, the volume phase transition temperature is tuned and essential properties, such as glucose diffusion kinetics, thermosensitivity, and cytocompatibility are evaluated. In addition, the self-cleaning functionality is demonstrated through thermally driven cell detachment from the membranes in vitro.

Graphical abstract

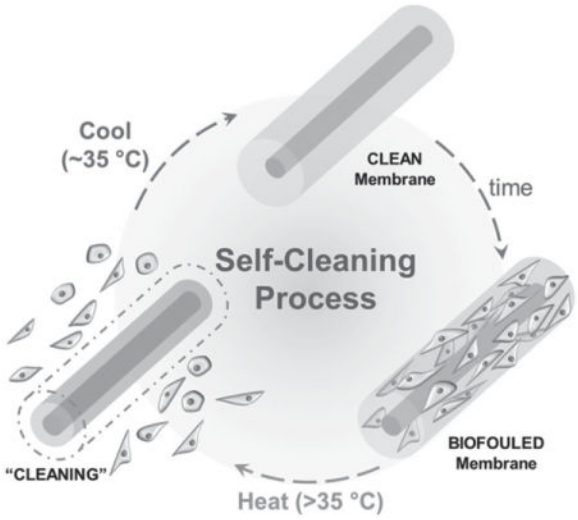

Keywords

biosensors; hydrogels; poly(*N*-isopropylacrylamide); self-cleaning; thermoresponsive

1. Introduction

Continuous glucose monitoring (CGM) is critical for the reduction of short- and long-term complications associated with diabetes.[1,2] A subcutaneously implanted glucose biosensor could provide CGM, but the problem of membrane biofouling must be resolved to ensure long-term efficacy.[3,4] Membrane biofouling is the product of the foreign body reaction in which biosensor implantation triggers the accumulation of proteins and cells.[5] By compromising glucose diffusion to the housed sensor, membrane biofouling severely limits the lifetime and sensitivity of transdermal and subcutaneous glucose biosensors. In order to minimize biofouling, membranes relying on a passive (i.e., antifouling) strategy have been most widely studied, including those based on poly(ethylene glycol) diacrylate (PEG-DA) hydrogels,[6] poly(tetrafluoroethylene) (PTFE),[7] e-PTFE,[7,8] poly(vinyl alcohol) (PVA) hydrogels,[9] polyhydroxyethyl-methacrylate (PHEMA) hydrogels,[10] and poly-L-lactic acid (PLLA).[11] In contrast, we have reported "self-cleaning membranes" based on poly(*N*-isopropylacrylamide) (PNIPAAm) hydrogels which utilize an active (i.e., foul-releasing) mechanism to physically remove attached cells.[12–14] PNIPAAm hydrogels are

thermoresponsive, deswelling and reswelling when heated above and cooled below their volume phase transition temperature (VPTT, ≈33–35 °C), respectively.[15,16] This process has been used for the thermally modulated release of cultured cells in vitro.[17–20] Most recently, we evaluated a PNIPAAm double network nanocomposite (DNNC) membrane as a candidate for a glucose biosensor self-cleaning membrane.[12] This membrane was comprised of an interpenetrating, asymmetrically crosslinked PNIPAAm matrix with polysiloxane nanoparticles (≈200 nm diameter) embedded during formation of the first network.[21] In the current study, we sought to create a superior self-cleaning membrane with a double network (DN) design based on PNIPAAm and an electrostatic co-monomer, 2-acrylamido-2-methylpropane sulfonic acid (AMPS) (Figure 1).

As previously reported,[22] we prepared DN hydrogels comprised of a tightly crosslinked, ionized first network [P(NIPAAm-*co*-AMPS)] containing variable levels of AMPS (100:0–25:75 wt% ratio of NIPAAm:AMPS) and a loosely crosslinked, interpenetrating second network [PNIPAAm]. AMPS is a strong electrolyte whose sulfonate groups undergo complete dissociation over a wide pH range.[23,24] Irrespective of AMPS content, the VPTT of these DN hydrogels was shown to be nearly unchanged versus conventional PNIPAAm hydrogels. Thus, while the VPTT of the P(NIPAAm-*co*-AMPS) first network was predictably increased due to the presence of the hydrophilic AMPS comonomer,[25,26] the "PNIPAAm-only" second network was able to produce the PNIPAAm hydrogel-like VPTT for the DNs. While conveniently not producing a change to the VPTT, the presence of AMPS in the first network produced improvements in other properties versus conventional SN PNIPAAm hydrogels including extent of swelling, thermosensitivity, and compressive strength. These properties were expected to promote glucose diffusion, self-cleaning, and the ability to withstand mechanical forces associated with implantation and indwelling.

Towards establishing their utility as self-cleaning membranes for implanted glucose biosensors, this study sought to tune the VPTT and assess key properties of P(NIPAAm-*co*-AMPS)/PNIPAAm DN membranes. First, the VPTT of the DN membranes was raised to above 35 °C, the temperature of the subcutaneous tissue of the wrist[27,28] and the expected location of an implanted biosensor. This would render the membrane swollen in the off-state (i.e., no heating), thereby maximizing glucose diffusion. To induce self-cleaning, the membrane would deswell upon transdermal heating above the VPTT (i.e., on-state). It is known that copolymerization of NIPAAm with a hydrophilic comonomer raises the VPTT of the hydrogel.[29,30] We have shown that small amounts (1–2 wt%) of *N*-vinylpyrrolidone (NVP) comonomer (based on NIPAAm wt) elevated the VPTT of the PNIPAAm-based DNNC[12] to ≈38 °C. Thus, NVP was likewise incorporated into the second network of the DN membranes reported herein. Second, glucose diffusion through planar DN membranes was experimentally measured at temperatures above and below the VPTT. Third, glucose diffusion lag time was calculated for DN membranes in the form of a cylindrical rod (≈1.5 mm × 5 mm, diameter × length), a geometry and size considered suitable for implantation. A finite-element model was utilized to estimate lag time to achieve equilibrium with the external environment of varying glucose concentrations. Given its impact on self-cleaning, thermosensitivity was assessed in terms of diameter change of DN membrane cylinders with thermal cycling above and below the VPTT. Finally, thermally modulated cell release from the surfaces of DN membranes was evaluated.

2. Experimental Section

2.1. Materials

NIPAAm (97%), AMPS (97%), PEG-DA (MW 575 g mol^{-1}) and *N*-vinylpyrrolidone (NVP) were obtained from Sigma–Aldrich. *N,N′*-methylenebisacrylamide (BIS, 99%) was purchased from ACROS. Chemical structures of all aforementioned materials are provided in Figure S1 in the Supporting Information. 2-Hydroxy-2-methyl-1-phenyl-propan-1-one (DAROCUR 1173) was purchased from Ciba Specialty Chemicals. 1-[4-(2-Hydroxyethoxy)-phenyl]-2-hydroxy-2-methyl-1-pro-pane-1-one (Irgacure 2959) was purchased from BASF. Rat dermal fibroblast cells and growth medium (R116–500) were obtained from Cell Applications. Lactate dehydrogenase (LDH) cytotoxicity assay kit was obtained from Pierce. Phosphate-buffered saline (PBS, 1X, pH 7.4, without calcium and magnesium) was obtained from Mediatech, Inc. Fetal bovine serum (FBS, Hyclone) was obtained from Fisher Scientific. Mesenchymal progenitor cells (10T1/2) were obtained from the American Type Culture Collection. Antibiotic antimycotic solution (100X) (stabilized bioreagent sterile filtered with 10 000 units of penicillin and 10 mg of streptomycin A), sodium bicarbonate ($NaHCO_3$), and Dulbecco's Modified Eagle's Medium (DMEM) (1000 mg dL^{-1} glucose and L-glutamine without Na_2CO_3 and phenol red) were purchased from Sigma–Aldrich. For hydrogel fabrication and other experiments, deionized water (DI H_2O) with a resistance of 18 MΩ·cm (Cascada LS MK2, Pall) was used. Cell culture media was made from a combination of antibiotic antimycotic solution (100X) (stabilized bioreagent sterile filtered with 10 000 units of penicillin and 10 mg of streptomycin A), $NaHCO_3$, DMEM (1000 mg dL−1 glucose and L-glutamine without sodium bicarbonate and phenol red), and FBS mixed into DI water. The pH was adjusted with 1 M HCl and 1 M NaOH, verified with a pH meter (420 A+, Orion; electrode 5990-30, Cole-Parmer), and sterilized by 0.2 μm filtration (sterile 90 mm filter unit, Nalgene Filtration Products).

2.2. Preparation of Non-Thermoresponsive PEG-DA Hydrogels

Precursor solutions were formed by vortexing DI H_2O, PEG-DA (100% v/v), and DARACUR 1173 (1% v/v) for 1 min.

Planar Sheets—Planar hydrogel sheets (≈1 mm thick per electronic caliper) were prepared by pipetting the precursor solution between two clamped glass slides (75 × 50 mm) separated by polycarbonate spacers (1 mm thick) and exposing the mold to longwave ultraviolet (UV) light (UVP UV-Transilluminator, 6 mW cm^{-2}, λ_{peak} = 365 nm) for 30 s at room temperature (RT). Hydrogel sheets were removed from their molds, rinsed with DI H_2O, and soaked in a Petri dish containing DI H_2O (60 mL) for 24 h.

Cylinders—Cylindrical hydrogels (≈3 mm × 5 mm, diameter × length per electronic caliper) were prepared by pipetting the precursor solution into a hollow cylindrical glass mold (inside diameter ≈2.5 mm, length = 10 mm) with one end sealed by Parafilm. After sealing the other end of the mold, it was likewise exposed to longwave UV-light as above at RT for 3 s. The cylindrical hydrogel was removed from the mold, rinsed with DI H_2O, and immersed in a Petri dish containing DI H_2O (60 mL) for 24 h. A clean razor blade was used to equally trim the ends to achieve a cylindrical length of 5 mm.

2.3. Preparation of Thermoresponsive DN Hydrogels

The "first network precursor solution" was formed with NIPAAm monomer, AMPS monomer (100:0, 75:25, 50:50 and 25:75 wt% NIPAAm:AMPS), BIS crosslinker, Irgacure-2959 photoinitiator and DI water. In a 50 mL round bottom (rb) flask equipped with a Teflon-covered stir bar, NIPAAm & AMPS (total weight of 1.0 g), BIS (0.04 g), and Irgacure 2959 (0.08 g) were dissolved in DI H_2O (7.0 mL). The "second network precursor solution" was formed by combining NIPAAm (6.0 g), NVP (0.96 g), BIS (0.012 g), Irgacure 2959 (0.24 g), and DI H_2O (21.0 mL). DN hydrogels are denoted as "*DN-X%*" where *X%* equals the wt% of AMPS in the first network's NIPAAm:AMPS wt% ratio (Table 1).

Planar Sheets—Planar hydrogel sheets (≈1 mm thick post-swelling) were produced by pipetting the first network precursor solution into a mold consisting of two clamped glass slides (75 × 50 mm) separated by 0.5 mm (for *DN-75%* and *DN-50%)* or 1 mm (for *DN-25%* and *DN-0%)* thick polycarbonate spacers. Thinner molds were utilized for *DN-75%* and *DN-50%* to account for their greater post-cure swelling.[22] The mold was then immersed in an ice water bath (≈7 °C) and exposed to longwave UV light for 30 min. The resulting "single network" (SN) PNI-PAAm or P(NIPAAm-*co*-AMPS) sheet was removed from the mold, rinsed with DI H_2O, and then soaked in DI H_2O at RT for 2 d with daily water changes. The SN sheet was then transferred into a covered Petri dish containing the second network precursor solution for 48 h at 2 °C. Next, the SN hydrogel sheet was placed into a rectangular mold (≈1 mm thick), photocured for 30 min in an ice water bath, and finally soaked in DI H_2O as above. These specimens were used to measure VPTT.

Cylinders—Cylindrical hydrogels (≈2.5–5.5 mm × 5 mm, diameter × length) were prepared by pipetting the precursor solution into a cylindrical glass mold [inside diameter ≈1 mm (for *DN-75%* and *DN-50%)* or ≈2.5 mm (for *DN-25%* and *DN-0%*), length = 10 mm] as above. The mold was immersed in an ice water bath and exposed for 30 min to longwave UV light. Cylindrical hydrogels were removed from their molds, rinsed with DI H_2O, and soaked in a Petri dish containing DI H_2O for 2 d at RT with daily water changes. The SN cylindrical hydrogel was then transferred into a Petri dish containing the second network precursor solution for 48 h at 2 °C. Next, the cylindrical hydrogel was placed into a cylindrical mold [diameter ≈2.5 mm (for *DN-75%* and *DN-50%*) or ≈6 mm (*DN-25%* and *DN-0%*), length = 10 mm], submerged in an ice water bath, exposed for 10 min to longwave UV light, and soaked in DI H_2O as above. A clean razor blade was used to trim ends to achieve a cylindrical length of 5 mm.

2.4. VPTT

The VPTT of swollen hydrogels was determined by differential scanning calorimetry (DSC, TA Instruments Q100). Water swollen hydrogels were blotted with a Kim Wipe and a small piece was sealed in a hermetic pan. After cooling to −50 °C, the temperature was increased to 50 °C and immediately returned to −50 °C at a rate of 3 °C min^{-1} for two continuous cycles. The resulting endothermic phase transition peak was characterized by the initial temperature at which the endotherm starts (T_o) and the peak temperature of the endotherm (T_{max}). Reported data are from the second cycle to ensure any thermal history has been

erased and to simulate the *n*th heating cycle during multiple continuous cycles, such as intended for this application.

2.5. Glucose Diffusion

Planar hydrogel strips (1 cm × 1 cm × ≈1 mm) were placed in a side-by-side diffusion cell (PermeGear) positioned atop a stir plate. The donor chamber contained 3 mL of glucose solution (≈1000 mg dL^{-1}), and the receptor chamber contained 3 mL of DI H_2O. Chamber solutions were stirred with Teflon-coated stir bars (800 rpm) to maintain constant solution concentrations. A water jacket maintained the designated temperature (35 and 40 °C) throughout the system. Every 10 min (for a total time of 3 h), 50 μL aliquots were removed via pipet from each chamber and glucose concentration was determined with a YSI 2700 Select Biochemistry Analyzer (YSI Incorporated). The diffusion coefficient (*D*) values were calculated using Fick's second law of diffusion after applying the assumptions that each solution maintained a uniform concentration and that the concentration of each element at the hydrogel membrane surface was equal to that in the bulk volume of each chamber.

2.6. Glucose Diffusion Lag Time

COMSOL Multiphysics software (COMSOL, Inc.) was used to develop a computational model of the glucose diffusion lag time for the DN hydrogels. The model utilized a time-dependent transport of diluted species study in which the rate of glucose diffusion through a geometric cylinder (1.5 mm × 5 mm, diameter × length) was analyzed. Model assumptions included the absence of backwards flux and a constant external glucose concentration. As used in our previous model,[12] the maximum and minimum free tetrahedral mesh element size were chosen as 0.382 and 0.0249 mm, respectively, to define the finite-element analysis. The simulation began with an initial internal glucose concentration of 0 mg dL^{-1} inside the DN hydrogel and initial external glucose levels of 60, 80, 160, and 300 mg dL^{-1}. The average glucose concentration within the cylindrical hydrogel was assessed every second for 1 h for each external glucose concentration. The diffusion lag time was defined as the time required for the hydrogel internal glucose concentration to reach 95% of the external glucose concentration.

2.7. Thermosensitivity

Three cylindrical DN hydrogels of each composition (≈2.5–5.5 mm × 5 mm, diameter × length) were vertically attached to a single Petri dish with a small amount of optical adhesive (Norland Optical Adhesive 61) to the base of one end. To hydrate the affixed cylinders, the Petri dish was filled with DI H_2O for at least 12 h at RT prior to thermally cycling. The Petri dish was positioned atop a heating plate under a DSLR camera (Canon Rebel T3i) with a 50 mm macro lens. Images were taken every 5 min as the hydrogels were thermally cycled between 25 and 40 °C for five cycles. The average rate of heating to 40 °C was ≈0.7 °C min^{-1}, and passive cooling to 25 °C occurred at a rate of ≈0.22 °C min^{-1}. Thus, each cycle consisted of a 1 h heating period followed by 1 h of passive cooling. Cylinder diameters were analyzed by ImageJ software.

2.8. Cytocompatibility

DN hydrogel cytocompatibility was assessed by measuring LDH concentrations released by rat dermal fibroblasts 24 h after cell seeding versus that of two cytocompatible controls, a PEG-DA hydrogel as well as tissue culture plastic (i.e., polystyrene, PS). Planar DN and PEG-DA hydrogel sheets were prepared as described above. Three 6 mm discs were punched from the sheet (≈1 mm thick) and then sterilized by immersion in 80% EtOH for 45 min. The hydrogel discs were then washed 3X (30 min each) with sterile PBS, submerged in PBS for 24 h, and subsequently transferred to a sterile 24-well plate. Next, rat dermal fibroblast cells suspended in rat fibroblast growth medium, were seeded onto each hydrogel disc and also into the empty tissue culture plastic wells at a concentration of ≈6500 cells cm^{-2}. Cells were incubated for 24 h at ≈37 °C with 5% CO_2. Finally, the media from each well was extracted and assessed for LDH level per the manufacture's protocol. The relative LDH activity was calculated by normalizing DN sample absorption to that of PS.

2.9. Cell Adhesion and Release

All DN planar hydrogels (≈20 mm diameter, ≈1 mm thickness) were transferred to a 12-well plate and soaked in PBS (2 d) and then sterilized by UV-irradiation overnight. Before seeding, all hydrogels were soaked in DMEM supplemented with 40% FBS and antibiotics for 1 h at RT (i.e., in their swollen state, $T <$ VPTT). Next, the media was removed and mouse mesenchymal progenitor 10T1/2 cells (suspended in fresh media containing 10% FBS) were seeded on the surface of the hydrogels at 25 000 cells cm^{-2}. After 5 h of incubation at 30 °C (i.e., swollen state; $T <$ VPTT), initial cell attachment was imaged immediately after removal from incubation using a Zeiss Axiovert 40C microscope (Carl Zeiss, Germany). A PS well plate dish served as a positive cell-adhesive control. To observe cell release, a transparent heating pad (Minco) was equipped to the microscope stage and controlled via LabView using a thermistor feedback system. The specimen was transferred to the temperature controlled stage and the thermistor was placed in the media above the gel to regulate the temperature. The specimen was heated from 30 °C ($T <$ VPTT) to 40 °C ($T >$ VPTT) at a rate of ≈1–2 °C min^{-1} to induce deswelling. After reaching 40 °C, the hydrogel was air cooled at ≈1–2 °C min^{-1} to RT to induce reswelling. Sequential heating and cooling cycles were immediately repeated with images captured at each swollen state at ≈25–30 °C.

3. Results and Discussion

3.1. VPTT

Thermoresponsive DN hydrogel membrane compositions are recorded in Table 1. DN hydrogels are denoted as "*DN-X%*" where *X%* equals the wt% of AMPS in the first network's NIPAAm:AMPS wt% ratio. As previously reported,[22] in the absence of the hydrophilic NVP comonomer, the VPTTs of DNs prepared with 100:0–75:25 (NIPAAm:AMPS) in the first network were 31.6–32.4 °C (T_o) and 32.9–34.0 °C (T_{max}). Thus, when implanted at the subcutaneous body temperature of the wrist ($T \approx$ 35 °C), these membranes would be deswollen in the off-state (i.e., no heating) which was anticipated to reduce glucose diffusion. Thus, in this work, a small amount of NVP comonomer (2 wt% based on total NIPAAm monomer weight) was incorporated into the second network to increase the VPTT to 35.7–36.0 °C (T_o) and 39.3–40.4 °C (T_{max}) (Table S1 and Figure S2).

3.2. Glucose Diffusion

The glucose diffusion coefficient (D) was assessed by examining glucose diffusion through each DN membrane when sandwiched between side-by-side diffusion cell systems. Measurements were performed at 35 °C (T < VPTT; swollen) and 40 °C (T > VPTT; deswollen), representing subcutaneous body temperature and an elevated temperature used to trigger self-cleaning, respectively. Fick's second law of diffusion, Equation (1), was used to calculate the diffusion coefficients at each temperature:

$$\frac{\partial c}{\partial t} = D\frac{\partial^2 c}{\partial x^2} \quad (1)$$

where c is the concentration within the hydrogel, t is the time, D is the diffusion coefficient, and x is the diffusion distance.[31–34] The above equation may be modified based on the assumption that each solution preserved a uniform concentration and that each element concentration was equal at the hydrogel membrane surface as in the bulk volume of each chamber. The simplified equation, Equation (2), is:

$$Q_t = \frac{ADC_1}{L}\left(t - \frac{L^2}{6D}\right) \quad (2)$$

where Q_t is the overall quantity of glucose transferred through the hydrogel until the specific time, t, A refers to the hydrogel area exposed to the donor or receiving chambers, C_1 is the initial solute concentration of the donor chamber, and L is the measured membrane thickness.

Values of D are reported in Table 1. At 35 °C (T < VPTT), the DN membranes were at the swollen state. Glucose diffusion increased with higher AMPS content in the first network with values of D increasing from 1.82 ± 0.02 × 10^{-6} (*DN-0%*) to 2.21 ± 0.02 × 10^{-6} (*DN-75%*). This is attributed to an increase in electrostatic repulsive forces that give rise to a more swollen membrane.[22] Glucose diffusion for DN membranes was enhanced versus that of a PEG-DA (MW 575 g mol^{-1}) membrane (D = 1.59 ± 0.42 × 10^{-6} cm^2 s^{-1}) which have been noted not to significantly inhibit glucose diffusion.[35] Furthermore, dermal and epidermal values of D have been reported as 2.64 ± 0.42 × 10^{-6} and 0.075 ± 0.05 × 10^{-6} cm^2 s^{-1}, respectively.[36] Thus, all DN membranes' D values fall within the functional range in their swollen state. When heated to 40 °C (T > VPTT), the DN membranes became deswollen. Expectedly, this reduced glucose diffusion as indicated by the decreased values of D. Overall, these results verify satisfactory glucose diffusion through the DN membranes in the swollen state. However, during deswelling, glucose measurements for any of these membranes would likely be prohibited.

3.3. Glucose Diffusion Lag Time

A COMSOL Multiphysics computational model was utilized to determine the theoretical glucose diffusion lag time for the DN cylindrical membranes (1.5 mm × 5 mm, diameter ×

length). The simulation utilized an initial glucose quantity within the hydrogel of 0 mg dL^{-1}. Subsequently, four different glucose concentrations (60, 80, 160, and 300 mg dL^{-1}), which represent low, normal, high, and very high physiological glucose levels,[37] were applied to the cylinders. With these conditions, the average glucose concentration within the hydrogel cavity was calculated every second for 1 h (Table 1 and Figure 2). For *DN-0%*, an average lag time of 19.01 ± 0.22 min was calculated. However, as AMPS content was increased, lag time decreased and was only 15.48 ± 0.15 min for *DN-75%*. The increase in swelling[22] may be responsible for the decreased lag time. Physiological lag times upward of 15 min have been reported between glucose changes in the interstitial fluid (ISF) and in the blood.[38–42] However, to further reduce the lag time, the cylinder diameter may be reduced. If a lag time of less than 5 min is desired, the required maximum diameters were also calculated using this diameter is decreased from 1.5 mm to ≈417 μm.

3.4. Thermosensitivity

Considered suitable geometry and size for an implanted glucose biosensor, DN membranes were prepared as cylinders (≈2.5–5.5 mm × 5 mm, diameter × length). The extent, rate, and consistency at which a cylindrical hydrogel deswells and reswells upon cyclically heating (T > VPTT) and cooling (T < VPTT) is critical for affecting cell detachment. Thus, the thermosensitivity of hydrogels was determined by measuring diameter change of vertically affixed cylinders during thermal cycling. Over a 10 h period, cylinders were subjected to five thermal cycles, each consisting of heating (≈0.70 °C min^{-1}) to 40 °C for 1 h and cooling (≈0.22 °C min^{-1}) to 25 °C for 1 h. During each thermal cycle, a consistent change in diameter was observed (Figure 3 and Table 1). The consistency in diameter change is essential for controlled and steady self-cleaning behavior. In addition, the maximum percentage change in diameter (from a swollen to deswollen state) increased with AMPS content. Thus, *DN-75%* was the most thermosensitive, exhibiting a change diameter of 33.5% ± 1.0%.

3.5. Cytocompatibility

For feasibility as a self-cleaning membrane for implanted glucose biosensors, the DN hydrogels must display cytocompatibility. This was assessed via LDH activity assays (Figure S3, Supporting Information). LDH is a cytosolic enzyme released into the media upon cellular apoptosis or necrosis and thus can be used to assess cellular toxicity.[43] LDH levels were measured 24 h post-seeding. LDH levels observed for all DN membranes were statistically similar to that of non-cytotoxic PEG-DA hydrogel and tissue culture plastic (i.e., PS). These results indicate the low cytotoxicity of DN membranes.

3.6. Cell Adhesion and Release (“Self-Cleaning”)

The self-cleaning ability of DN hydrogel membranes was evaluated both in terms of the initial levels of cell adhesion in the swollen state as well as the release of adhered cells upon thermal cycling (Figure 1). PS tissue culture plastic was used as a cell adhesive control. In order to obtain sufficient levels of adhered cells, DN membranes were first conditioned in DMEM (40% FBS) for 1 h. Preconditioning of a surface with protein is conventionally used to promote adhesion of cells.[44] Moreover, protein adsorption precedes cellular adhesion for a surface upon implantation.[45] Seeded cells (in fresh media containing 10% FBS), were

incubated on the surface of swollen DN membranes at 30 °C. After 5 h, cell adhesion was examined (Figure 4). In the case of the cell-adhesive PS, cells exhibited typical spread morphology indicative of attachment. For DN membranes, higher levels of AMPS contributed to an increased degree of cell adhesiveness. For *DN-0%* (i.e. no AMPS), a round cell morphology was observed, suggesting poor attachment. In fact, numerous cells were observed to migrate across this surface owing to a lack of attachment. Cell adhesiveness remained low for *DN-25%* but notably increased for *DN-50%.* This observation is attributed to the known greater affinity of cells to negatively charged versus neutral surfaces.[46–48] Somewhat unexpectedly, despite higher levels of AMPS, *DN-75%* exhibited reduced cell adhesiveness, with most cells displaying a round morphology and only few spread cells observed. This may be the result of increased hydration which accompanies this higher AMPS content,[22] resulting in more hydrophilic, surfaces which reduce initial cell adhesion.[17,49]

Following observation of initial cell attachment to swollen DN membranes, specimens were subjected to successive thermal cycling from 30 °C (swollen state) to 40 °C (deswollen state). Images were captured after two cycles upon return to their swollen state (Figure 5). For all *DN-0%, DN-25%*, and *DN-75%* membranes, a round cell morphology was maintained after thermal cycling. For *DN-50%*, two thermal cycles induced cells to change from a spread to a round morphology with some cells floating across membrane surface, indicating effective cellular detachment. Likewise for *DN-75%*, after two thermal cycles, all cells displayed a round morphology, with many floating across the surface. For the PS control, cells remained spread and attached, confirming that thermal cycling of the cells on a traditional, non-thermoresponsive surface did not cause detachment.

4. Conclusions

To explore their potential as self-cleaning membranes for implanted glucose biosensors, we refined and evaluated key properties of DN membranes based on PNIPAAm and electrostatic comonomer, AMPS. The DN membranes were comprised of a tightly crosslinked, ionized first network [P(NIPAAm-*co*-AMPS)] containing variable levels of AMPS (100:0–25:75 wt % ratio of NIPAAm:AMPS) and a loosely crosslinked, interpenetrating second network [PNIPAAm]. The VPTT was adjusted to ≈38 °C by incorporation of NVP comonomer into the second network. In this way, the DN membranes were swollen in the off-state when implanted in the subcutaneous tissue of the wrist and glucose diffusion was maximized.

Experimentally measured glucose diffusion coefficients (D) were shown to increase with AMPS content. In addition, when considered as implantable cylinders (1.5 mm × 5 mm, diameter × length), calculated glucose diffusion lag time decreased with AMPS content. Enhanced glucose diffusion with AMPS content is attributed to the corresponding increase in membrane swelling.[22] Glucose diffusion was best for *DN-75%* (i.e., 25:75 wt% NIPAAm:AMPS in first network) with D equaled to $2.21 \pm 0.02 \times 10^{-6}$ cm^2 s^{-1} and lag time equaled to 15.48 ± 0.15 min. In comparison, our previously reported PNIPAAm-based DNNC membrane displayed relatively diminished glucose diffusion properties ($D = 1.88 \pm 0.01 \times 10^{-6}$ cm^2 s^{-1} and lag time ≈19 min). Should a lag time of less than 5 min be desired, the diameter of *DN-75%* could be reduced to 417 μm. Thermally driven diameter

change of cylindrical DN membranes was shown to be consistent over multiple cycles with the greatest maximum change in diameter observed for *DN-75%* (33.5 ± 1.0%). After 5 h in the swollen state, cells showed little or no attachment to *DN-0%*, *DN-25%*, and *DN-75%* whereas significant attachment was shown for *DN-50%.* Thus, while cells were adhesive to the more negatively charged surface of *DN-50%*, the higher hydration (swelling) of *DN-75%* diminished adhesion. Still, after only two thermal cycles, all cells on each DN membrane composition assumed a round morphology, indicative of cell detachment. These properties along, with their enhanced mechanical behavior,[22] make these DN hydrogels excellent candidates for a self-cleaning membrane for implanted glucose biosensors.

Supplementary Material

Refer to Web version on PubMed Central for supplementary material.

Acknowledgments

Funding from the NIH/NIDDK (1R01DK095101-01A1) is gratefully acknowledged. We thank Prof. Michael McShane (Texas A&M University) for use of his YSI 2700 Select Biochemistry Analyzer. We also thank Prof. Mariah Hahn (Rensselaer Polytechnic Institute) for the gift of the 10T1/2 cells.

References

1. Shamoon H, Duffy H, Fleischer N, Engel S, Saenger P, Strelzyn M, Litwak M, Wylie-Rosett J, Farkash A, Geiger D, Engel H, Fleischman J, Pompi D, Ginsberg N, Glover M, Brisman M, Walker E, Thomashunis A, Gonzalez J. New Engl J Med. 1993; 329:977. [PubMed: 8366922]
2. Nathan DM, Cleary PA, Backlund JYC, Genuth SM, Lachin JM, Orchard TJ, Raskin P, Zinman B. New Engl J Med. 2005; 353:2643. [PubMed: 16371630]
3. Wisniewski N, Reichert M. Colloid Surf B: Biointerfaces. 2000; 18:197. [PubMed: 10915944]
4. Frost M, Meyerhoff ME. Anal Chem. 2006; 78:7370. [PubMed: 17128516]
5. Anderson JM. Annu Rev Mater Res. 2001; 2001:81.
6. Quinn CAC, Connor RE, Heller A. Biomaterials. 1997; 18:1665. [PubMed: 9613815]
7. Bota PCS, Collie AMB, Puolakkainen P, Vernon RB, Sage EH, Ratner BD, Stayton PS. J Biomed Mater Res A. 2010; 95:649. [PubMed: 20725970]
8. Updike SJ, Shults MC, Gilligan BJ, Rhodes RK. Diabetes Care. 2000; 23:208. [PubMed: 10868833]
9. Sharkawy AA, Klitzman B, Truskey GA, Reichert WM. J Biomed Mater Res A. 1998; 40:586.
10. Marshall AJ, Ratner BD. AIChE J. 2005; 51:1221.
11. Koschwanez HE, Yap FY, Klitzman B, Reichert WM. J Biomed Mater Res A. 2008; 87A:792.
12. Abraham AA, Fei R, Cote GL, Grunlan MA. ACS Appl Mater Interfaces. 2013; 5:12832. [PubMed: 24304009]
13. Gant R, Abraham A, Hou Y, Grunlan MA, Cote GL. Acta Biomater. 2010; 6:2903. [PubMed: 20123136]
14. Gant R, Hou Y, Grunlan MA, Cote GL. J Biomed Mater Res A. 2009; 90:695. [PubMed: 18563815]
15. Hoffman AS, Afrassiabi A, Dong LC. J Control Release. 1986; 4:213.
16. Zhang J, Pelton R, Deng Y. Langmuir. 1995; 11:2301.
17. Okano T, Yamada N, Okuhara M, Sakai H, Sakurai Y. Biomaterials. 1995; 16:297. [PubMed: 7772669]
18. Kobayashi J, Okano T. Sci Tech Adv Mater. 2010; 11:1.
19. Yang J, Yamato M, Nishida K, Ohki T, Kanzaki M, Sekine H, Shimizu T, Okano T. J Control Release. 2006; 116:193. [PubMed: 16890320]
20. Tang Z, Akiyama Y, Okano T. Polymers. 2012; 4:1478.

21. Fei R, George JT, Park J, Grunlan MA. Soft Matter. 2012; 8:481. [PubMed: 23293658]
22. Fei R, George JT, Park J, Means AK, Grunlan MA. Soft Matter. 2013; 9:2912.
23. Travas-Sejdic J, Easteal A. Polym Gels Netw. 1998; 5:481.
24. Melekaslan D, Okay O. Polymer. 2000; 41:5737.
25. Turan E, Demirci S, Caykara T. J Polym Sci B: Polym Phys. 2008; 46:1713.
26. Feil H, Bae YH, Feijen J, Kim SW. Macromolecules. 1993; 26:2496.
27. Montgomery LD, Williams BA. Ann Biomed Eng. 1976; 4:209. [PubMed: 984529]
28. Werner J, Buse M. J Appl Physiol. 1988; 65:1110. [PubMed: 3182480]
29. Erbil C, Aras S, Uyanik N. J Polym Sci A: Polym Chem. 1999; 37:1847.
30. Feil H, Bae YH, Feijen J, Kim SW. Macromolecules. 1993; 26:2496.
31. Hannoun BJ, Stephanopoulos G. Biotech Bioeng. 1986; 28:829.
32. Teixeira JA, Mota M, Venancio A. Chem Eng J Biochem Eng J. 1994; 56:B9.
33. Venancio A, Teixeira JA. Biotech Tech. 1997; 11:183.
34. Zhang W, Furusaki S. Biochem Eng J. 2001; 9:73.
35. Quinn CP, Pishko MV, Schmidtke DW, Ishikawa M, Wagner JG, Raskin P, Hubbell JA, Heller A. Am J Physiol. 1995; 269:E155. [PubMed: 7631771]
36. Khalil E, Kretsos K, Kasting GB. Pharm Res. 2006; 23:1227. [PubMed: 16715366]
37. Tuchin, VV. Handbook of Optical Sensing of Glucose in Biological Fluids and Tissues. CRC Press; Boca Raton: 2009. p. xxxii
38. Aussedat B, Dupire-Angel M, Gifford R, Klein JC, Wilson GS, Reach G. Am J Physiol Endocrinol Metabol. 2000; 278:E716.
39. Baker DA, Gough DA. Anal Chem. 1996; 68:1292. [PubMed: 8651496]
40. Heise T, Koschinsky T, Heinemann L, Lodwig V. Diab Technol Therap. 2003; 5:563.
41. Rebrin K, Steil GM. Diab Technol Ther. 2000; 2:461.
42. Rebrin K, Steil GM, van Antwerp WP, Mastrototaro JJ. Am J Physiol. 1999; 277:E561. [PubMed: 10484370]
43. Renner K, Amberger A, Konwalinka G, Kofler R, Gnaiger E. Biochim Biophys Acta. 2003; 1642:115. [PubMed: 12972300]
44. Grinnell F, Feld MK. J Biolog Chem. 1982; 257:4888.
45. Frost M, Meyerhoff ME. Anal Chem. 2006; 78:7370. [PubMed: 17128516]
46. Kishida A, Iwata H, Tamada Y, Ikada Y. Biomaterials. 1991; 12:786. [PubMed: 1799655]
47. Haraguchi K, Takehisa T, Ebato M. Biomacromolecules. 2006; 7:3267. [PubMed: 17096560]
48. Schneider GB, English A, Abraham M, Zaharias R, Stanford C, Keller J. Biomaterials. 2004; 25:3023. [PubMed: 14967535]
49. Lydon MJ, Minett TW, Tighe BJ. Biomaterials. 1985; 6:396. [PubMed: 4084641]

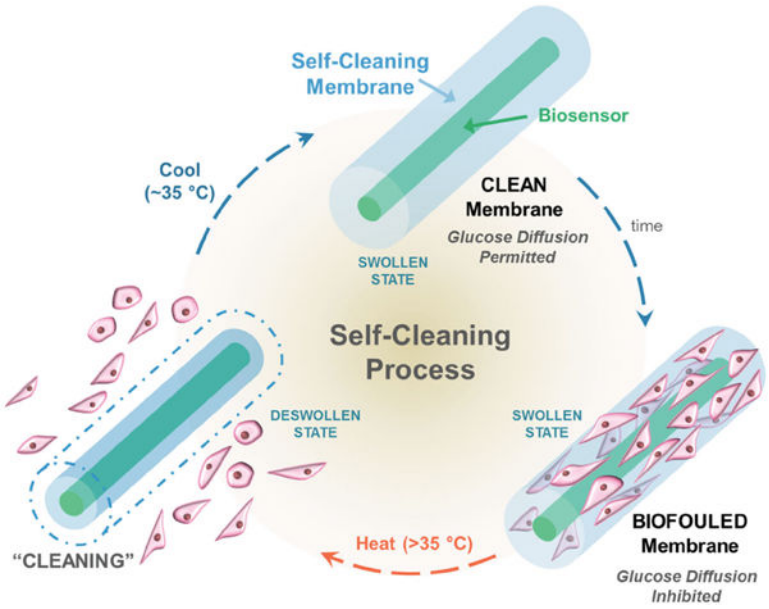

Figure 1.

"Self-cleaning" glucose biosensor (green inner cylinder) based on thermoresponsive double network (DN) P(NIPAAm-*co*-AMPS)/PNIPAAm hydrogels (blue outer cylinder). Thermal cycling above and below the VPTT induces deswelling (bottom left) and reswelling (top), respectively, leading to cell release (pink) and restoration of glucose diffusion.

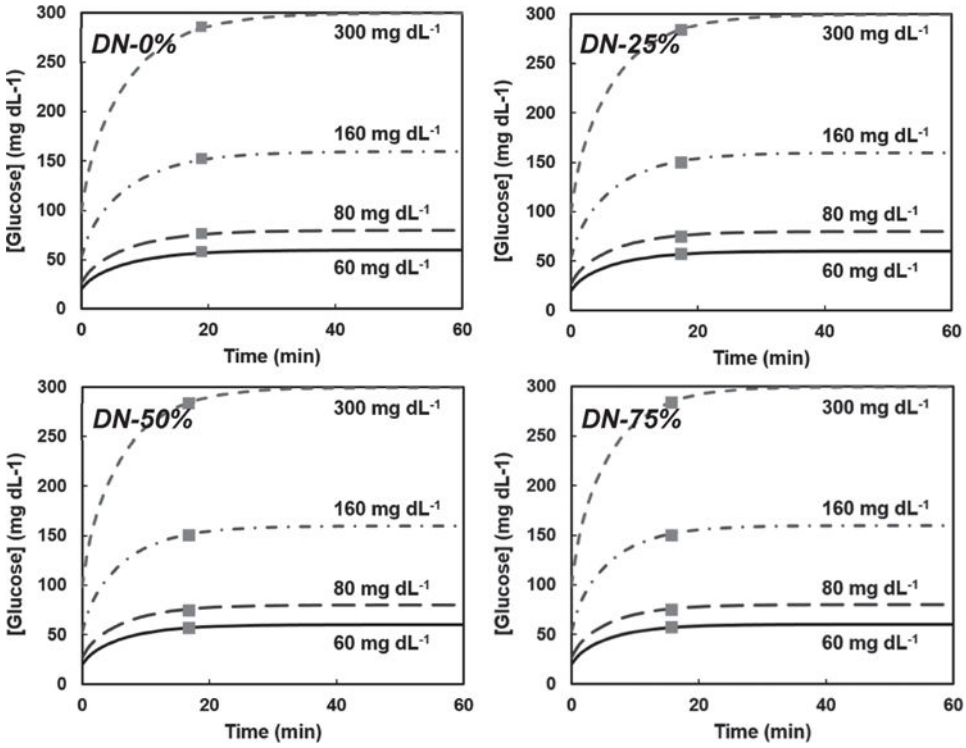

Figure 2.

Calculated average glucose concentration inside cylindrical hydrogels (1.5 × 5 mm) at 35 °C for constant environment glucose levels of 60, 80, 160, and 300 mg dL^{-1}. The glucose diffusion lag time (gray square) marks when the average internal hydrogel glucose concentration is 95% to that of the external environment.

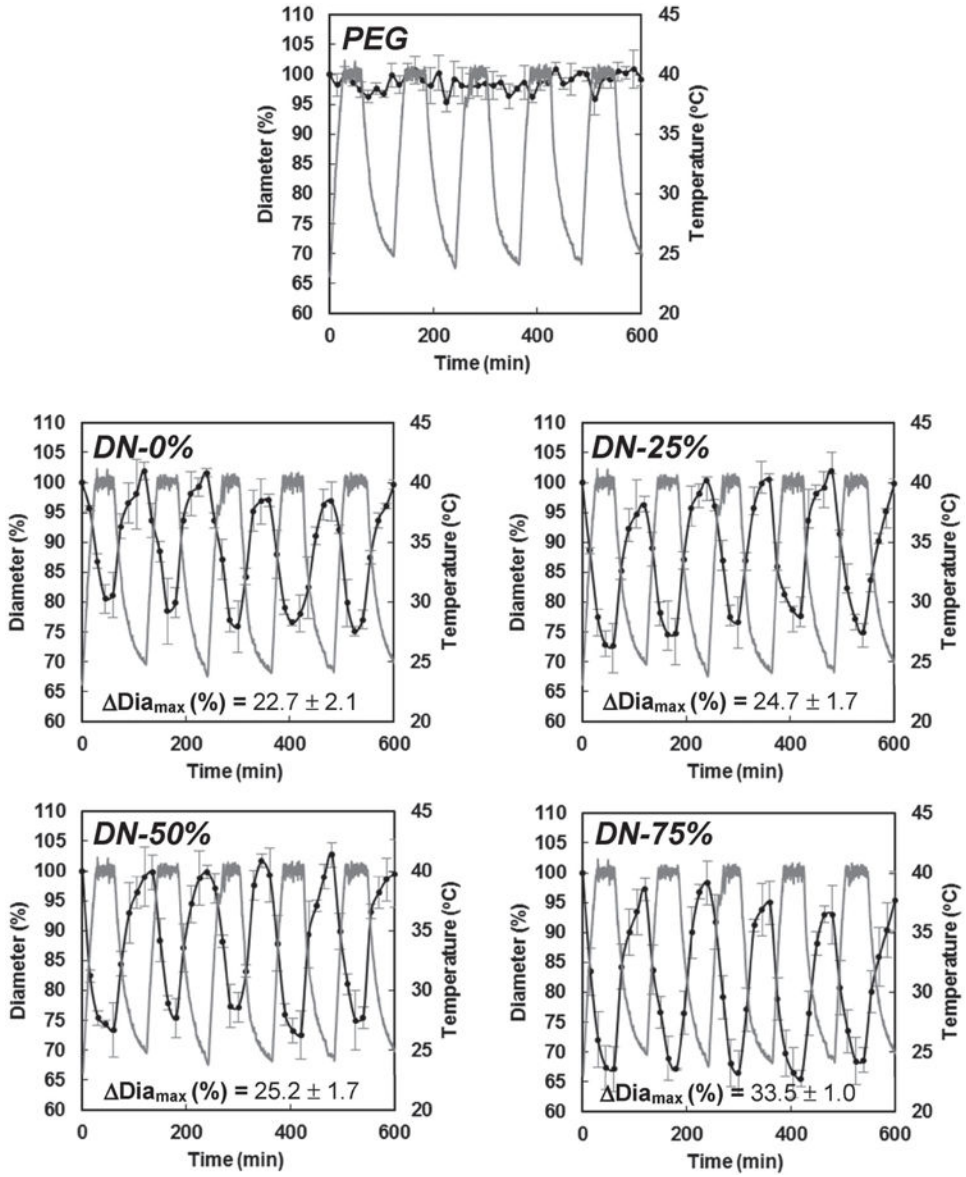

Figure 3.

Diameter change during thermal cycling of vertically affixed hydrogel cylinders (10 h time period). Diameter change (black) and temperature change (gray).

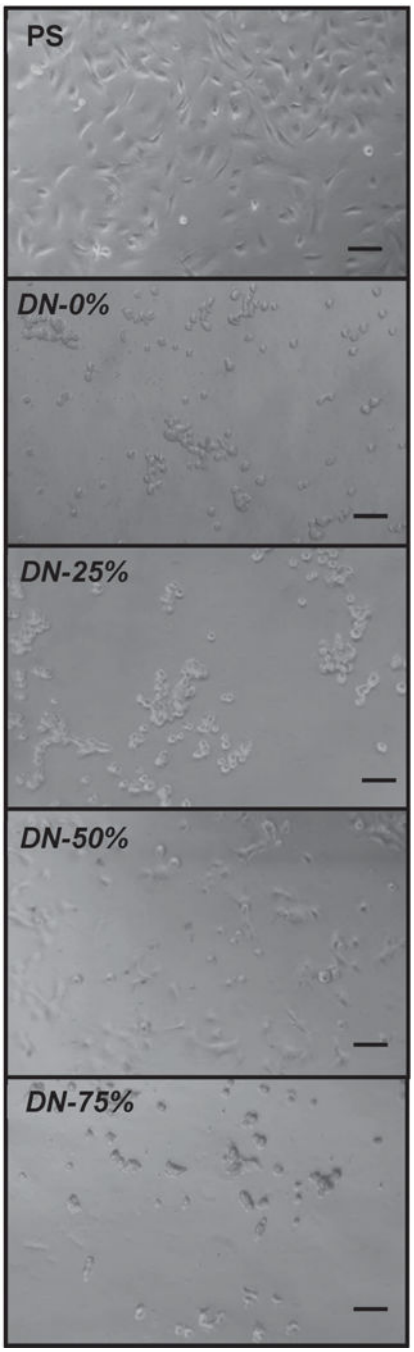

Figure 4.
Representative images of PS tissue culture plastic and DN membranes following 5 h culture with 10T1/2 cells at 30 °C (swollen state) prior to thermal cycling. Scale bar = 100 μm.

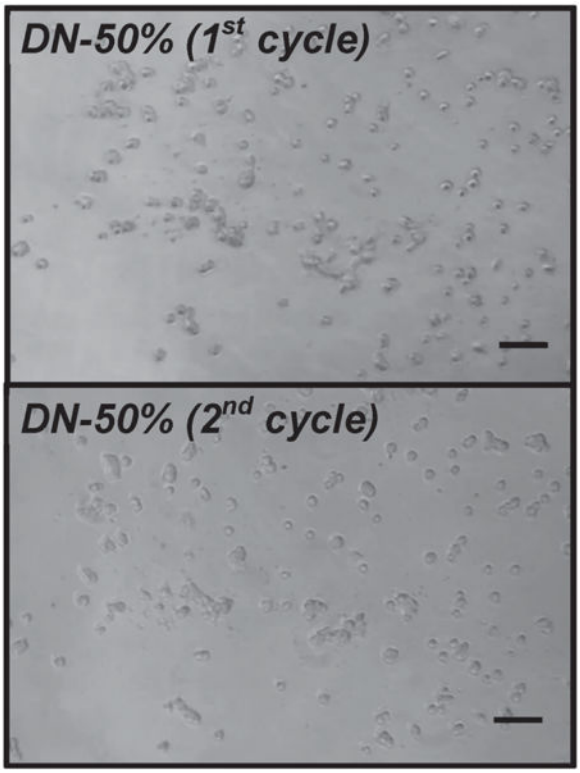

Figure 5.

Representative images of 10T1/2 cell detachment from *DN-50%* with thermal cycling: (top) after first thermal cycle and return to the swollen state, some cells switch from a spread to round morphology, indicative of detachment and (bottom) after second thermal cycle and return to the swollen state, all cells adopt a round morphology. Scale bars = 100 μm.

Table 1

Glucose diffusion coefficient (D) of hydrogels below and above the VPTT.

DN notation	Firstnetwork: NIPAAm:AMPS (wt%)	Temperature [°C]	Membrane behavior	Average D [$cm^2\ s^{-1}$]	Glucose diffusion lag time [min]	Maximum diameter [μm] for 5 min lag time	Maximum diameter change [%] (swollen to deswollen state)
DN-0%	100:0	35	Swollen	$1.82 \pm 0.02 \times 10^{-6}$	19.01 ± 0.22	346	22.7 ± 2.1
DN-25%	75:25	35	Swollen	$1.99 \pm 0.01 \times 10^{-6}$	17.29 ± 0.09	394	24.7 ± 1.7
DN-50%	50:50	35	Swollen	$2.06 \pm 0.03 \times 10^{-6}$	16.67 ± 0.26	403	25.2 ± 1.7
DN-75%	25:75	35	Swollen	$2.21 \pm 0.02 \times 10^{-6}$	15.48 ± 0.15	417	33.2 ± 1.0
DN-0%	100:0	40	Deswollen	$1.16 \pm 0.02 \times 10^{-6}$	–	–	(See above)
DN-25%	75:25	40	Deswollen	$0.66 \pm 0.02 \times 10^{-6}$	–	–	(See above)
DN-50%	50:50	40	Deswollen	$0.75 \pm 0.01 \times 10^{-6}$	–	–	(See above)
DN-75%	25:75	40	Deswollen	$1.04 \pm 0.03 \times 10^{-6}$	–	–	(See above)